Nonlin. Processes Geophys. Discuss., https://doi.org/10.5194/npg-2018-49
Manuscript under review for journal Nonlin. Processes Geophys.
Discussion started: 5 December 2018

Nonlinear Processes in Geophysics
Open Access
Discussions

Can the Nucleation Phase be Generated on a Sub-fault Linked to the Main Fault of an Earthquake?

Jeen-Hwa Wang

Institute of Earth Sciences, Academia Sinica , P.O. Box 1-55, Nangang, Taipei, TAIWAN email: jhwang@earth.sinica.edu.tw

(submitted toNonlinear Processes in Geophysics on November 3, 2018)

Abstract. We study the effects of seismic coupling, friction, viscous, and inertia on earthquake nucleation based on a two-body spring-slider model in the presence of thermal-pressurized slip-dependent friction and viscosity. The stiffness ratio of the system to represent seismic coupling is the ratio of coil spring *K* between two sliders and the leaf spring *L* between a slider and the background plate and denoted by $s=K/L$. The *s* is not a significant factor in generating the nucleation phase. The masses of the two sliders are m_1 and m_2, respectively. The frictional and viscous effects are specified by the static friction force, f_o, the characteristic displacement, U_c, and viscosity coefficient, η, respectively. Numerical simulations show that friction and viscosity can both lengthen the natural period of the system and viscosity increases the duration time of motion of the slider. Higher viscosity causes lower particle velocities than lower viscosity. The ratios $\gamma=\eta_2/\eta_1$, $\phi=f_{o2}/f_{o1}$, $\psi=U_{c2}/U_{c1}$, and $\mu=m_2/m_1$ are four important factors in influencing the generation of a nucleation phase. When $s>0.17$, $\gamma>1$, $1.15>\phi>1$, $\psi<1$, and $\mu<30$, simulation results exhibit the generation of nucleation phase on slider 1 and the formation of *P* wave on slider 2. The results are consistent with the observations and suggest the possibility of

generation of nucleation phase on a sub-fault.

Keywords: nucleation phase, two-body spring-slider model, stiffness ratio, thermal-pressurized slip-dependent friction, viscosity

Nonlin. Processes Geophys. Discuss., https://doi.org/10.5194/npg-2018-49
Manuscript under review for journal Nonlin. Processes Geophys.
Discussion started: 5 December 2018

Nonlinear Processes in Geophysics
Open Access
Discussions

1 **Introduction**

The presence of nucleation phase before the *P* waves (see Fig. 1) was suggested by early theoretical studies (e.g., Andrews, 1976; Brune, 1979; Dieterich, 1986, 1992; Das and Scholz, 1981) and laboratory experiments (Dieterich, 1979; Ohnaka et al., 1987). Some studies (Scholz et al., 1972; Dieterich, 1981; Ohnaka and Yamashita, 1989; Ohnaka, 1992; Ohnaka and Kuwahara, 1990; Kato et al., 1994; Roy and Marone, 1996; Lu et al., 2010; Latour et al., 2013; Kaneko et al., 2016) also indicated that the nucleation process behaves like a transition from quasi-static slip (without the inertial effect) to (unstable) dynamic motion (with the inertial effect) when the slip speeds become high enough to make the inertial effect dominate frictional resistance under some conditions. The study of this phase is a basic problem of earthquake physics and also important for early warming, prediction, and hazard assessment of earthquakes.

Umeda (1990) first recognized the nucleation phase in velocity seismograms. Since then, numerous seismologists also observed the nucleation phases (e.g., Iio, 1992, 1995; Ellsworth and Beroza, 1995; Beroza and Ellsworth, 1996; Mori and Kanamori, 1996; Ruiz et al., 2017). There is a debate concerning the correlation between the duration time, T_D, of nucleation phase and the magnitude, *M*, of the earthquake occurring immediately after the nucleation phase. Ellsworth and Beroza (1995) and Beroza and Ellsworth (1996) assumed a positive correlation of T_D to *M*. Whereas, Mori and Kanamori (1996) observed independence of the *P* waves on the shape of nucleation phase in a large magnitude range. Ellsworth and Beroza (1998) confirmed the observation by Mori and Kanamori (1996).

Friction and viscosity are two major factors in controlling the complicated earthquake rupture processes including nucleation (see Wang, 2016; and cited

Nonlin. Processes Geophys. Discuss., https://doi.org/10.5194/npg-2018-49
Manuscript under review for journal Nonlin. Processes Geophys.
Discussion started: 5 December 2018

Nonlinear Processes in Geophysics
Discussions
Open Access

references therein). Analytic solutions and numerical simulations for exploring the nucleation phase have made based on the infinite dislocation models, crack models, and spring-slider models by using different friction laws (see Beeler, 2004; Tal et al., 2018; Wang, 2016, 2017a; and cited references therein). Iio (1992, 1995) stressed that the nucleation phase cannot be interpreted by any theoretical source model with a constant kinematic friction and a constant rupture velocity. Mori and Kanamori (1996) claimed that any model having a similar initial rupture can describe the nucleation phases of earthquakes of all sizes, and thus it is difficult to estimate the magnitude of an earthquake just from its nucleation phase. They also stressed that curvature seen in the nucleation phases is caused by anelastic attenuation.

Some theoretical studies based on the Burridge-Knopoff spring-slider model (Burridge and Knopoff, 1967), from which the two-body model used in this study is simplified, are briefly described here. Brantut et al. (2011) concluded that metamorphic dehydration influences the nucleation of unstable slip and could be an origin for slow-slip events in subduction zones. Ueda et al. (2014, 2015) and Kawamura et al. (2018) pointed out that the nucleation process includes the quasi-static initial phase, the unstable acceleration phase, and the high-speed rupture phase (i.e., a mainshock) and recognized two kinds of nucleation lengths, i.e., L_{sc} and L_c which are affected by model parameters, yet not by the earthquake size. The L_{sc} related to the initial phase exists only for a weak frictional instability regime; while the L_c associated with the acceleration phase exist for both weak and strong instability regimes. They also found that in the initial phase up to L_{sc}, the sliding velocity is of order the plate speed, while at a certain stage of the acceleration phase it becomes higher and thus can be observed.

Although the frictional effect on earthquake nucleation has been long and widely studied as mentioned above, the studies of viscous effect on earthquake ruptures are rare. The viscous effect mentioned in Rice et al. (2001) was actually an implicit factor which is included within the direct effect of rate- and state-dependent friction law. Wang (2017a) took viscosity into account for studying the nucleation phase by assuming a temporal change of high viscosity to low viscosity during an earthquake rupture based on a one-body spring slider model with thermal-pressurized slip-weakening friction. His results in a temporal variation from nucleation phases to *P* wave and the amplitude of *P* wave, which is associated with the earthquake magnitude, does not depend on the duration time of the former.

As mentioned above, the nucleation process behaves like a transition from quasi-static slip (without the inertial effect) to (unstable) dynamic motion (with the inertial effect) when the slip speeds become high enough to make the inertial effect dominate frictional resistance under some conditions. This assumes that the inertial effect must be taken into account.

In most of studies, both the nucleation phase and the *P* wave are assumed to occur on the same fault. There is an interesting question: Can the nucleation phase happen on a sub-fault which links to the main fault of an earthquake? In order to answer this question, in this work I will explore the frictional, viscous, and inertial effects on the generation of nucleation phase on a fault and then the transition from it to the *P* wave on the other based on a two-body spring-slider model, which is used to approach an earthquake fault (see Galvanetto, 2002; Turcotte, 1992), by considering the two sliders to be two segments of an earthquake fault,. The friction force caused by thermal pressurization is slip-weakening and the viscosity is represented by an explicit parameter. In addition, it is significant to consider the inertial effect on the earthquake nucleation because of the existence of transition from quasi-static motion

Nonlin. Processes Geophys. Discuss., https://doi.org/10.5194/npg-2018-49
Manuscript under review for journal Nonlin. Processes Geophys.
Discussion started: 5 December 2018

Nonlinear Processes in Geophysics
Open Access
Discussions

to dynamic ruptures from observations and laboratory experiments. The study on inertial effect on nucleation phase is rare, even though this effect is implicitly included in the thermal-pressurized friction used by Brantut et al. (2011). Here, the inertial effect will be taken into account.

2 Two-body Spring-slider Model

The two-body spring-slider model (Fig. 2) consists of two sliders of mass m_i (i=1, 2) and three springs. The detailed description of the model can be seen in Wang (2017b) and only briefly explained here. The equation of motion of the system is

$$m_1 d^2u_1/dt^2 = K(u_2-u_1)-L_1(u_1-v_Pt)-F_1(u_1)-\Phi(v_1) \quad \text{(1a)}$$

$$m_2 d^2u_2/dt^2 = K(u_1-u_2)-L_2(u_2-v_Pt)-F_2(u_2)-\Phi(v_2). \quad \text{(1b)}$$

The u_i (i=1, 2) is the displacement of the slider measured from its initial equilibrium position along the x-axis. The K is the strength of the coil spring between two sliders and the L_i (i=1, 2) is the strength of the leaf spring to yield the driving force on the i-th slider from a moving plate with a constant speed v_P. Considering the two sliders to be two segments of a single earthquake fault, the coupling between the moving plate and a slider could be equal for the two sliders, thus giving $L_1=L_2=L$. $F_i(u_i)$ (i=1, 2) is the frictional force on the i-th slider. Wang (2013) took $F(u)=F_o exp(-u/u_c)$, where F_o and u_c are, respectively, the static friction force and characteristic slip displacement, to study earthquake dynamics. This friction force is slip-weakening and caused by the adiabatic-undrained-deformation (AUD)-type thermal pressurization (Rice, 2006). An example of the variations of $F(u)$ versus u for F_o=1 N and u_c=0.1,

Nonlin. Processes Geophys. Discuss., https://doi.org/10.5194/npg-2018-49
Manuscript under review for journal Nonlin. Processes Geophys.
Discussion started: 5 December 2018

0.3, 0.5, 0.7, and 0.9 m is displayed in Fig. 3. *F(u)* decreases with increasing u, and the decreases rate is higher for smaller u_c than for larger u_c. This indicates that the force drop decreases with increasing u_c for the same final displacement. The $\Phi(v_i)$, where $v_i=du_i/dt$ is the particle velocity, is a velocity-dependent viscous force. According to Stokes' law, Wang (2016) suggested the viscous force to be $\Phi=Cv$, where $C=6\pi R\upsilon$ (with a unit of N(m/s)$^{-1}$) is the damping coefficient of a sphere of radius R in a fluid of viscosity υ (Kittel et al. 1968). The two sliders rest in an equilibrium state at time $t=0$. Note that this model addresses only the strike-slip component and, thus, cannot completely represent earthquake ruptures, which also consist of transpressive components. Nevertheless, simulation results of this model can still provide significant information on earthquake ruptures.

Substituting the friction and viscous laws into Equation (1) leads to

$$m_1 d^2u_1/dt^2=K(u_2-u_1)-L(u_1-v_Pt)-F_{o1}exp(-u_1/u_{c1})-C_1du_1/dt \quad (2a)$$

$$m_2 d^2u_2/dt^2=K(u_1-u_2)-L(u_2-v_Pt)-F_{o2}exp(-u_2/u_{c2})-C_2du_2/dt \quad (2b)$$

To deal with the problem easily, it is usual to normalize Equation (2) based on the normalization parameters. Wang (1995) defined the stiffness ratio, s, to be the ratio of K to L, i.e., $s=K/L$. Wang (2017b) defined the normalization parameters for Equation (2). However, in his study he took $m_1=m_2$, and thus he did not consider the cases with different values of m_1 and m_2. While, in this study m_2 could be larger than m_1 for showing the inertial effect. Hence, the parameters normalizing Equation (2) are: $m_1=m$, $m_2=\mu m$, $F_{o1}=F_o$, $F_{o2}=\phi F_o$, $D_o=F_o/L$, $\omega_{o1}=\omega_o=(L/m)^{1/2}$, $\omega_{o2}=\mu^{-1/2}\omega_o$, $\tau=\omega_o t$, $u_{c1}=u_c$, $u_{c2}=\psi u_c$, $U_{c1}=u_c/D_o$, $U_{c2}=\psi u_c/D_o$, $f_{o1}=f_o=F_o/D_o$, $f_{o2}=\phi f_o$, $\eta_1=C_1\omega_o/L$,

$\eta_2=C_2\mu^{-1/2}\omega_o/L$, $\gamma=\eta_2/\eta_1$, and $V_P=v_P/D_o\omega_o$. Defining $U_i=u_i/D_o$ and $V_i=dU_i/d\tau$ leads to $du_i/dt=[F_o/(mL)^{1/2}]dU_i/d\tau$ and $d^2u_i/dt^2=(F_o/m)d^2U_i/d\tau^2$. Inserting these normalization parameters with f_o=1 into Equation (2) results in:

$$d^2U_1/d\tau^2=s(U_2-U_1)-(U_1-V_P\tau)-exp(-U_1/U_{c1})-\eta_1 dU_1/d\tau \quad (3a)$$

$$d^2U_2/d\tau^2=[s(U_1-U_2)-(U_2-V_P\tau)-\phi exp(-U_2/U_{c2})-\eta_2 dU_2/d\tau]/\mu. \quad (3b)$$

Let $y_1=U_1$, $y_2=U_2$, $y_3=dU_1/d\tau$, and $y_4=dU_2/d\tau$. Equation (3) can be re-written as four first-order differential equations:

$$dy_1/d\tau=y_3 \quad (4a)$$

$$dy_2/d\tau=y_4 \quad (4b)$$

$$dy_3/d\tau=-(s+1)y_1+sy_2-exp(-y_1/U_{c1})-\eta_1 y_3+V_P\tau \quad (4c)$$

$$dy_4/d\tau=[sy_1-(s+1)y_2-\phi exp(-y_2/\psi U_{c1})-\gamma\eta_1 y_4+V_P\tau]/\mu. \quad (4d)$$

Since it is difficult to analytically solve Equation (4), only numerical simulations using the fourth-order Runge-Kutta method (see Press et al., 1986) is performed in this study. Note that the sliders are restricted to move only along the positive direction, that is, $V_i\geq0$ and $U_i\geq0$ (i=1, 2).

3 Numerical Simulations

Nonlin. Processes Geophys. Discuss., https://doi.org/10.5194/npg-2018-49
Manuscript under review for journal Nonlin. Processes Geophys.
Discussion started: 5 December 2018

Before performing numerical simulations, it is necessary to consider the acceptable values of model parameters. Strong coupling can make the two sliders move almost simultaneously. Hence, in order to allow independent motion for each slider, the value of s should be small. Numerical tests (Wang, 2017b) show weak coupling as s<5 and strong coupling as s≥5 for a two-body spring-slider system. Hence, s<5 is considered in this study. In general, v_P is ~10^{-9} m/s and thus V_P is ~10^{-9} when $D_o\omega_o$ is an order of magnitude of 1 m/sec. Simulation results could be influenced by using various time steps, $\delta\tau$. Practical tests suggest that simulation results show numerical stability when $\delta\tau$<0.05. The time step is taken to be $\delta\tau$=0.02 hereafter. When $V_P\tau=exp(-y_1/U_{c1})$ on slider 1 from Equation (4c), the force exerted from the moving plate is just equal to f_{oi}. Although in principle slider 1 can start to move under this condition, in practice the computation cannot go ahead because all values are zero. An initial force, δf, is necessary to kick off slider 1. Note that the value of δf can affect the computational results (Carlson et al., 1991). A very small value of δf cannot enforce slider 1 to move; while a large one will dominate the whole computation process. Numerical tests show that δf=10^{-3} is appropriate for numerical simulations.

Numerical simulations are made under various values of model parameters for showing the effects caused by seismic coupling, friction, viscosity, and inertial effect. Simulation results are displayed in Figures 4−10 which include the time variations in V/V_{max} (in the left-hand-side panels) and U/U_{max} (in the right-hand-side panels).

The results for the effect due to seismic coupling are displayed in Fig. 4 where the values of s are: (a) for s=0.06, (b) for s=0.12, (c) for s=0.30, and (d) for s=0.48 when f_{o1}=1.0 and f_{o2}=1.0 (with ϕ=1), U_{c1}=0.5 and U_{c2}=0.5 (with ψ=1), and η_1=0 and η_2=0 (with γ=1). First, it is necessary to examine the lower-bound value of s for yielding strong enough coupling between the two sliders. Numerical tests exhibit that slider 2 cannot move for s<0.06 when other model parameters are equal on the two sliders. Hence, s=0.06 is almost the lower bound of seismic coupling for most of simulations. On the other hand, numerical tests suggest that when s>0.48, the solid and dashed lines are coincided. This means that large s having strong seismic coupling leads to almost simultaneous motions of the two sliders. Hence, the value of s is taken to be 0.48 in Figs. 5−7, and 9 to explore which factor can separate the motions of the two sliders.

Figures 5−8 display the results due to different values of viscosity on the two sliders when other parameters are fixed: (a) for γ=0.00 (i.e., η_2=0), (b) for γ=0.01 (i.e., η_2=0.1), (c) for γ=0.05 (i.e., η_2=0.5), and (d) for γ=0.10 (i.e., η_2=1) when η_1=10. In Fig. 5 the values of other model parameters are μ=1, η_1=10, s=0.48, f_{o1}=1.0 and f_{o2}=1.0 (with ϕ=1), and U_{c1}=0.5 and U_{c2}=0.5 (with ψ=1). The figure displays the presence of the P wave on slider 2. Numerical tests reveal that the P wave on slider 2 cannot be generated especially for γ≥0.05 when η_1>70, and the solutions are just like Figure 4 when η_1<5. Hence, η_1 is taken to be 10 in Figs. 6−10. The simulation results to exhibit the effect due to different static friction strengths on the two sliders, are displayed in Fig. 6, where the values of other model parameters are μ=1, η_1=10, s=0.48, f_{o1}=1.0 and f_{o2}=1.1 (with ϕ=1.1), and U_{c1}=0.5 and U_{c2}=0.5 (with ψ=1). The figure exhibits the presence of a nucleation phase on slider 1. Numerical tests exhibit that when ϕ>1.15, the P wave on slider 2 cannot be generated. Hence, ϕ is taken to be 1.1 in Figs. 7−10. The simulation results to exhibit the effect due to different characteristic displacements on the two sliders are displayed in Fig. 7, where the values of other model parameters are μ=1, η_1=10 s=0.48, f_{o1}=1.0 and f_{o2}=1.1 (with ϕ=1.1), and U_{c1}=0.5 and U_{c2}=0.1 (with ψ=0.2). The figure shows the presence of a nucleation phase on slider 1. Numerical tests exhibit that when U_{c1}>0.5, the P wave

Nonlin. Processes Geophys. Discuss., https://doi.org/10.5194/npg-2018-49
Manuscript under review for journal Nonlin. Processes Geophys.
Discussion started: 5 December 2018

on slider 2 cannot be generated. Hence, U_{c1} is taken to be 0.5 in Figs. 8−10. In order to consider weaker seismic coupling on the simulated waveforms, smaller s is taken into account. Numerical tests exhibit that when s<0.17, the P wave on slider 2 cannot be generated. Hence, s is also taken to be 0.17 in Fig. 8 where the values of other model parameters are μ=1, η_1=10, s=0.17, f_{o1}=1.0 and f_{o2}=1.1 (with ϕ=1.1), and U_{c1}=0.5 and U_{c2}=0.1 (with ψ=0.2).

Figures 9 and 10 display the results for the inertial effect due to different masses of the two sliders: (a) for μ=1, (b) for μ=5, (c) for μ=10, and (d) for μ=30 when η_1=10, f_{o1}=1.0 and f_{o2}=1.1 (with ϕ=1.1), U_{c1}=0.5 and U_{c2}=0.1 (with ψ=0.2), and η_1=10 and η_2=0 (with γ=0). The main difference between the two figures is the use of different values of seismic coupling: s=0.48 in Fig. 9 and s=0.17 in Fig. 10.

In the panels of Figs. 4−10, the simulation results for slider 1 and slider 2 are represented, respectively, by a solid line and a dotted line. Numerical results show that the values of V_{max} and U_{max} are: 0.456 and 1.355, respectively, in Fig. 4; 0.142 and 0.798, respectively, in Fig. 5; 0.226 and 0.766, respectively, in Fig. 6; 0.781 and 1.403, respectively, in Fig. 7; 0.903 and 1.778, respectively, in Fig. 8; 0.781 and 1.505, respectively, in Fig. 9; and 0.903 and 1.790, respectively, in Fig. 10.

4 Discussion

4.1 Seismic Coupling Effect

Figure 4 shows the simulation results when s=0.06, 0.12, 0.30, and 0.48 (upside down). In the left-hand-side panels for V/V_{max}, the dashed line separates from the solid line for small s, while the two lines are almost coincided for large s. This reflects the fact that seismic coupling between the two sliders increases with s. Meanwhile, the peak amplitude is larger at slider 2 than at slider 1. This is reasonable due to the directivity effect because the system moves from slider 1 to slider 2. However, this figure does not exhibit the existence of long-period nucleation phase. Hence, seismic coupling is not a significant factor in the generation of nucleation phase. From the right-hand-side panels for U/U_{max}, we can also obtain the same conclusion as mentioned above. In addition, the final displacements on the two sliders are almost equal.

4.2 Viscous Effect

Simulation results based on a one-body spring-slider model by Wang (2017a) show that a change of viscosity from a lager value to a small one in two time stages during slippage yields the nucleation phase and the *P* wave, respectively, in the first and second stages. Hence, in Fig. 5 the value of η_1 is set to be 10 and η_2 varies from 0 to 1 or γ varies from 0.0 to 0.1 for s=0.48 when the values of other parameters are the same as those in Fig. 4. The left-hand-side panels of Fig. 5 exhibit the presence of a short-time nucleation phase plus a smaller event on slider 1 and a larger event with a *P* wave on slider 2. Hence, there are two sub-events during the whole rupture process. The peak velocity of slider 2 decreases with increasing γ, yet not for slider 1. The peak velocity appears earlier on slider 2 than on slider 1. The occurrence time of the peak velocity of slider 2 slightly increases with γ. In addition, there are few events with low peak velocities after the main one on slider 2, and the number of small events decreases with increasing γ.

The predominant period and the peak velocity of slider 1 are, respectively, longer and smaller than those of slider 2. Of course, the differences decrease with increasing γ or η_2. Compared with Fig. 4, the predominant periods for the two sliders in Fig. 5 become longer due to the viscous effect. From Equation (1), the (dimensionless)

Nonlin. Processes Geophys. Discuss., https://doi.org/10.5194/npg-2018-49
Manuscript under review for journal Nonlin. Processes Geophys.
Discussion started: 5 December 2018

Nonlinear Processes in Geophysics
Discussions
Open Access
EGU

natural period is $T_{o1}=T_o=2\pi(m/L)^{1/2}$ for slider 1 and $T_{o2}=2\pi(\mu m/L)^{1/2}=\mu^{1/2}T_o$ for slider 2 when the two sliders are not linked together and friction and viscosity are both absent. When the two sliders are linked together, the natural period of each slider must be slightly different from T_{o1} or T_{o2}. When viscosity is included, the natural period is $T_1=T_{o1}/(1\text{-}C_1^2/4mL)^{1/2}=T_o/(1\text{-}\eta_1^2/4)^{1/2}$ for slider 1 and $T_2=T_{o2}/(1\text{-}C_2^2/4\mu mL)^{1/2}=\ \mu^{1/2}T_o/(1\text{-}\eta_2^2/4)^{1/2}$ for slider 2. Obviously, viscosity increases the natural period of oscillations of each slider and also depresses the peak velocity. The ratio of T_2 to T_1 is:

$$T_2/T_1=[\mu(4\text{-}\eta_1^2)/(4\text{-}\eta_2^2)]^{1/2}=[\mu(4\text{-}\eta_1^2)/(4\text{-}\gamma\eta_1^2)]^{1/2}. \quad (5)$$

Equation (5) shows that when $\mu>1$ and $\gamma>1$, we have $T_2>T_1$. When η_2 approaches 2, T_2 becomes infinity. Hence, $\eta_2=2$ is an upper bound of generating a normal *P* wave. The left-hand-side panels of Fig. 5 exhibits an increase in T_2 with η_2 or γ.

In the right-hand-side panels of Fig. 5, the displacement of slider 2 (displayed by a dashed line) first increases more rapidly than that of slider 1 (shown by a solid line) and finally two lines merge together, thus exhibiting the same final displacement on the two sliders.

Although we can see the existence of long-period waveform on slider 1 in Fig. 5, its peak velocity comes after that of a short-period *P* wave on slider 2. This does not exhibit transition from quasi-static motions to dynamic ruptures as shown from observations, and thus the whole waveform on slider 1 cannot be classified to be the nucleation phase. Hence, it is assumed that different values of viscosity coefficients on the two sliders are not the unique factor to yield the nucleation phase for the two-body model, and thus the differences in other model parameters between the two sliders must be taken into account.

4.3 Frictional Effect

The fictional effect includes two components: the static friction forces or the frictional strength (denoted by f_{o1} and f_{o2} on slider 1 and slider 2, respectively) and the characteristic displacements of friction law (represented by U_{c1} and U_{c2} on slider 1 and slider 2, respectively). First, we consider different values of s, f_{o1}, and f_{o2}. Simulation results are displayed in Fig. 6 where static friction forces are f_{o1}=1.0 and f_{o2}=1.1 (with ϕ=1.1) when other values of model parameters are the same as those in Fig. 5, i.e., s=0.48, U_{c1}=0.5 and U_{c2}=0.5 (with ψ=1), and (a) for γ=0.00 or η_2=0, (b) for γ=0.01 or η_2=0.1, (c) for γ=0.05 or η_2=0.5, and (d) for γ=0.10 or η_2=1 when η_1=10. The left-hand-side panels show the presence of a very long-duration nucleation phase on slider 1 in the front of the P wave on sider 2. After slider 2 stopped motion, slider 1 still moves and its peak velocity comes after that of slider 2. The occurrence time of the peak velocity slightly increases with γ. Although a bump appears in the waveform of slider 1, its peak velocity is much smaller than that of slider 2. Hence, unlike Fig. 5 there is almost only one event in the whole rupture process in Fig. 6. Meanwhile, the maximum value of peak velocity of Fig. 6 is higher than that of Fig. 5. In the right-hand-side panels of Fig. 6, the displacements of slider 1 (displayed by a solid line) and slider 2 (displayed by a dashed line) appear almost simultaneously and increase with time. The final displacement is higher on slider 2 than on slider 1, and the difference between the two final displacements decreases with increasing γ.

Tal et al. (2018) who studied numerically the effects of fault roughness with amplitude of b_r on the nucleation process of earthquakes in the presence of a rat- and state-dependent friction law. The roughness can yields local barriers and makes the

Nonlin. Processes Geophys. Discuss., https://doi.org/10.5194/npg-2018-49
Manuscript under review for journal Nonlin. Processes Geophys.
Discussion started: 5 December 2018

nucleation process complicated. They also found an increase in nucleation length with b_r. Considering a broad weak zone with a locally strong asperity on a fault plane, Shibazaki and Matsu'ura (1995) found that in the dynamic rupture of the asperity, there are aseismic slip and foreshock or pre-event, depending on the peak stress of the asperity, preceding the main rupture and the rupture of the asperity accelerates the nucleation of main rupture. This study indicates the influence of heterogeneous friction strengths on the generation of nucleation phase. Schmitt et al. (2015) considered the importance of time-dependent stress heterogeneity on nucleation. Although this factor is not taken into account in this study, the present study for different values of ϕ on the two sliders seems able to meet the results obtained by the three groups.

Secondly, we consider different values of U_{c1} and U_{c2}. Simulation results are displayed in Fig. 7 where the values of characteristic displacements are U_{c1}=0.5 and U_{c2}=0.1 (with ψ=0.2) and the values of other model parameters are the same as those in Fig. 6, i.e., s=0.48, f_{o1}=1.0 and f_{o2}=1.1 (with ϕ=1.1), and (a) for γ=0.00 or η_2=0, (b) for γ=0.01 or η_2=0.1, (c) for γ=0.05 or η_2=0.5, and (d) for γ=0.10 or η_2=1 when η_1=10. Like Fig. 6, the left-hand-side panels show the existence of a very long-duration nucleation phase on slider 1 in the front of the P wave on sider 2. After slider 2 stopped motion, slider 1 still moves and its peak velocity comes after that of slider 2. The occurrence time of the peak velocity slightly increases with γ. The maximum value of peak velocity of Fig. 7 is higher than that of Fig. 6. In addition, the predominant period of P wave on slider 2 is shorter in Fig. 7 than in Fig. 6. This might be due to a faster drop of friction force in Fig. 7 with shorter U_{c2} than in Fig. 6 with longer U_{c2}. Although a peak velocity appears in the waveform of slider 1, its amplitude is very much smaller than that of slider 2. Hence, unlike Fig. 5 there is

Nonlin. Processes Geophys. Discuss., https://doi.org/10.5194/npg-2018-49
Manuscript under review for journal Nonlin. Processes Geophys.
Discussion started: 5 December 2018

Nonlinear Processes in Geophysics
Open Access
Discussions

almost only one event in the whole rupture process of Fig. 7. In the right-hand-side panels of Fig. 7, the displacement of slider 1 (displayed by a solid line) first appears and increases with time; while the displacement of slider 2 (displayed by a dashed line) suddenly appears for a while after slider 1 moves and then jumps to its peak value in a short time. The final displacement is higher on slider 2 than on slider 1, and the difference between the two final displacements decreases with increasing γ.

Using an infinite elastic model with a slip-dependent friction, Ionescu and Campillo (1999) found the influence of the shape of the friction law and fault finiteness on the duration of nucleation phase and the duration varies when the fault length has the order of the characteristic length of the friction law. The present study is essentially consistent with their results.

Thirdly, it is necessary to consider the effect on the simulations due to weak seismic coupling (now s=0.17) between the two sliders when the values of other model parameters are the same as those in Fig. 7, i.e., f_{o1}=1.0 and f_{o2}=1.1 (with ϕ=1.1), and U_{c1}=0.5 and U_{c2}=0.1 (with ψ=0.2) , and (a) for γ=0.00 or η_2=0, (b) for γ=0.01 or η_2=0.1, (c) for γ=0.05 or η_2=0.5, and (d) for γ=0.10 or η_2=1 when η_1=10. Simulation results are displayed in Fig. 8. Like Figs. 6 and 7, there is a very long-duration nucleation phase on slider 1 in the front of the P wave on sider 2. After slider 2 stopped motion, slider 1 still moves and its peak velocity comes after that on slider 2. The peak velocity of slider 1 appears much later than that in Fig. 7. This might be due to a fact that it needs a longer time to trigger slider 2 due to weak coupling between the two sliders in Fig. 8. Meanwhile, the occurrence time of the peak velocity on slider 2 slightly increases with γ. From the values of peak velocity as mentioned above, the maximum value of peak velocity in Fig. 8 is higher than that in Fig. 7. This indicates that weaker coupling between two sliders can yield a higher peak velocity than stronger coupling. In addition, the predominant period of *P* wave on slider 2 is shorter in Fig. 8 than in Fig. 7. Although a peak velocity appears in the waveform of slider 1, its amplitude is very much smaller than that of slider 2. Unlike Fig. 5 there is almost only one event in the whole rupture process of Fig. 8.

In the right-hand-side panels of Fig. 8, the displacement of slider 1 (displayed by a solid line) first appears and increases with time; while the displacement of slider 2 (displayed by a dashed line) suddenly appears for a while after slider 1 moves and then jumps to its peak value in a short time span. The final displacement is higher on slider 2 than on slider 1, and the difference between the two final displacements decreases with increasing γ.

4.4 Inertial Effect

The inertial effect (represented by μ) on the earthquake nucleation is made for different masses of the two sliders, i.e., μ>1. Simulation results are displayed in Fig. 9 with s=0.48 and in Fig. 10 with s=0.48. In the two figures, the values of μ are: (a) for μ=1, (b) for μ=5, (c) for μ=10, and (d) for μ=30 when s=0.48, f_{o1}=1.0 and f_{o2}=1.1 (with ϕ=1.1), U_{c1}=0.5 and U_{c2}=0.1 (with ψ=0.2), and η_1=10 and η_2=0 (with γ=0). Like Figs. 6−8, Figs. 9 and 10 show the existence of very long-duration nucleation phases on slider 1 in the front of the *P* wave on sider 2. After slider 2 stopped moving, slider 1 still moves and its peak velocity comes after that on slider 2. The occurrence times of the peak velocity of both sliders 1 and 2 in Figs. 9 and 10 increase with μ and are almost similar to those in Figs. 7 and 8, respectively. The occurrence times of the peak velocity in Fig. 10 are longer than those in Fig. 9. This might be due to a fact that a longer time is needed to trigger slider 2 due to weak coupling between the two sliders in Fig. 10. Meanwhile, the predominant periods of the *P* wave on sider 2 increases with μ as expected. From the values of peak velocity as mentioned above, the maximum value of peak velocity of Fig. 10 is higher than that of Fig. 9. This indicates that that weaker coupling between two sliders can yield a higher peak velocity on slider 2 than stronger coupling. In addition, the peak velocity on slider 1 is lower than that on slider 2 and decreases with μ especially for small s. Although a peak velocity appears in the waveform of slider 1 in Figs. 9 and 10, its amplitude is much smaller than that of slider 1. Unlike Figure 5, there is almost only one event in the rupture process in Figs. 9 and 10.

In Figs. 9 and 10, the peak velocity of P wave decreases with increasing μ. Numerical tests exhibit that the P wave almost becomes a nucleation phase on slider 2 when μ>30. In the other word, the nucleation phase on slider 1 cannot trigger the P wave on slider 2 when the mass of the latter is 30 times larger than that of the former. When the densities and fault widths of the two sliders are equal, the fault length of slider 2 is 30 times longer than that of slider 1 when μ=30. Since the present model is a strike-slip (SS) one, the empirical relationship of earthquake magnitude, M, versus fault length, L, for the SS events is: $M=(5.16\pm0.13)+(1.12\pm0.08)log(L)$ (Wells and Coppersmith, 1994). When μ=30 or $L_2=30L_1$, the related magnitudes are M_1 for slider 1 and M_1+1.65 for slider 2. This means that a nucleation phase with a magnitude of M cannot trigger an earthquake with a magnitude of M+1.65.

In the right-hand-side panels of Figs. 9 and 10, the displacement of slider 1 (displayed by a solid line) first appears and increases with time; while the displacement of slider 2 (displayed by a dashed line) suddenly appears for a while after slider 1 moves and then jumps to its peak value in a short time span. The difference in final displacement between the two sliders slightly increases with μ and

Nonlin. Processes Geophys. Discuss., https://doi.org/10.5194/npg-2018-49
Manuscript under review for journal Nonlin. Processes Geophys.
Discussion started: 5 December 2018

Nonlinear Processes in Geophysics
Open Access
Discussions

is bigger for small *s* than for large *s*. The phenomenon that the final displacement of slider 1 is lower than that of slider 2 might be due to a fact that the force drop on slider 2 is higher than that on slider 1.

4.5 Some Comparisons with Other Studies

Numerical simulations of this study exhibit that the ratios $\gamma=\eta_2/\eta_1$, $\phi=f_{o2}/f_{o1}$, $\psi=U_{c2}/U_{cl}$, and $\mu=m_2/m_1$ are four important factors in influencing the earthquake rupture processes including the generation of nucleation phase, yet the seismic coupling s is a minor one. Except for the cases with equal values on the two sliders for the four ratios, the nucleation phase happens on slider 1 and the *P* wave appears on slider 2. When $\gamma>1$, $\phi=1$, $\psi=1$, and $\mu=1$, there is only a very short-duration nucleation phase and the P wave appears very soon after the generation of nucleation phase. This is inconsistent with Figure 1.

When $\gamma>1$, $\phi>1$, $\psi\geq1$, and $\mu=1$, there is a long-duration nucleation phase on slider 1, the *P* wave appears on slider 2 much lately after the generation of nucleation phase. Although the simulated waveforms are consistent with Fig. 1, the final displacement of nucleation phase on slider 1 is the same as that of the *P* wave on slider 2. This indicates equal values of total energy on the two sliders. It is questionable, because the energy of nucleation phase is lower than that of the mainshock from observations.

When $\gamma>1$, $\phi>1$, $\psi<1$, and $\mu=1$, the final displacement of nucleation phase is smaller than that of *P* wave. The difference in the amplitudes between the *P* wave and nucleation phase decreases with increasing *s*, increasing γ, or decreasing ψ. The simulated waveforms are consistent with Fig. 1. The results are reasonable, because the total energy on slider 1 is less than that on slider 2.

Nonlin. Processes Geophys. Discuss., https://doi.org/10.5194/npg-2018-49
Manuscript under review for journal Nonlin. Processes Geophys.
Discussion started: 5 December 2018

When γ>1, ϕ>1, and ψ<1, the peak velocity of slider 2 decreases with increasing μ, and becomes very small when μ>30, even though the final displacement of nucleation phase is still smaller than that of *P* wave. The degree of similarity of simulated waveforms of these cases (see Figs. 9 and 10) with Fig. 1 decreases with increasing μ. The upper-bound value of μ to yield transition from nucleation phase to the *P* wave from observations is 30. Consequently, the optimal conditions for generating the nucleation phase on slider 1 plus the *P* wave on slider 1 as displayed in Figure 1 and the results from other studies are γ>1, ϕ>1, ψ<1, and μ<30. Of course, there are upper-bound values for γ and ϕ and a lower-bound value for ψ as mentioned in the last section. Note that the upper-bound value of a ratio depends on the values of other ratios.

However, a difference between the present study and previous ones is that the nucleation phase appears on slider 1 and does not disappear after the presence of *P* wave on slier 2. This might be due to a use of a two-body model in this study and uses of a one-body or 1-D model is taken in others. Meanwhile, the mechanism (including friction and viscosity) to yield the transition from quasi-static motions to dynamic ruptures proposed in this study is the same as that in Wang (2017a), yet different from others who only considered the frictional effect. However, unlike Wang (2017a) the present simulation results cannot lead to the conclusion that the peak amplitude of *P* wave, which is associated with the earthquake magnitude, is independent upon the duration time of nucleation phase. In addition, the inertial effect was not taken into account by Wang (2017a).

Based on an infinite elastic model with slip-dependent friction, Shibazaki and Matsu'ura (1992) assumed that the transition process includes three phases: phase-I for the low quasi-static nucleation, phase-II for the onset of dynamic ruptured with

Nonlin. Processes Geophys. Discuss., https://doi.org/10.5194/npg-2018-49
Manuscript under review for journal Nonlin. Processes Geophys.
Discussion started: 5 December 2018

slow rupture growth in the absence of seismic-wave radiation, and phase-III for the high-speed rupture propagation with seismic-wave radiation. Shibazaki and Matsu'ura (1993) further found that the accelerating stage from phase-II to phase-III is related to the presence of nucleation phase in the front of the main *P* wave. Their results are similar to those obtained by Ueda et al. (2014, 2015) and Kawamura et al (2018). The results of this study and Wang (2017a) only show two stages which are comparable with the phase-II and phase-II stages proposed by Shibazaki and Matsu'ura (1992, 1993). From the analytic solutions of an infinite elastic model with a slip-dependent friction, Campillo and Ionescu (1997) expressed how the initiation phase determines the transition to the P wave and claimed that the transition is controlled by an apparent supersonic velocity of the rupture front. However, the present result does not seem to meet their conclusion. According to an infinite elastic model with rate- and state-dependent friction, Segall and Rice (2006) divided the weakening processes of ruptures into the nucleation regime dominated by rate and state frictional weakening and a transition regime to thermal pressurization. In the present study, the thermal-pressurized slip-weakening friction is considered during the whole rupture process and the results show a transition from the nucleation phase with smaller f_{o1} and U_{c1} on slider 1 to the *P* wave with larger f_{o2} and U_{c2} on slider 2. Hence, the present result could be only partly consistent with their conclusion.

5 Conclusions

We study the frictional and viscous effects on earthquake nucleation based on a two-body spring-slider model in the presence of thermal-pressurized slip-dependent friction and viscosity. The stiffness ratio of the system is the ratio of coil spring *K* between two sliders and the leaf spring *L* between a slider and the background plate

Nonlin. Processes Geophys. Discuss., https://doi.org/10.5194/npg-2018-49
Manuscript under review for journal Nonlin. Processes Geophys.
Discussion started: 5 December 2018

and denoted by $s=K/L$. The s is not a significant factor in generating the nucleation phase. The masses of the two sliders are m_1 and m_2, respectively. The frictional and viscous effects are specified by the static friction force, f_o, the characteristic displacement, U_c, and viscosity coefficient, η, respectively. Simulation results show that friction and viscosity can both lengthen the natural period of the system and viscosity increases the duration time of motion of the slider. Higher viscosity causes lower particle velocities than lower viscosity. The ratios $\gamma=\eta_2/\eta_1$, $\phi=f_{o2}/f_{o1}$, $\psi=U_{c2}/U_{cl}$, and $\mu=m_2/m_1$ are four important factors in influencing the generation of a nucleation phase. When $\gamma>1$, $\phi=1$, $\psi=1$, and $\mu=1$, the nucleation phase is generated on slider 1 and the P wave appear on slider 2. But, the P wave appears very soon after the generation of nucleation phase. When $\gamma>1$, $\phi>1$, $\psi\geq1$, and $\mu=1$, the P wave appears much lately after the generation of nucleation phase. When $\psi\geq1$, the final displacement of nucleation phase is almost equal to that of P wave. When $\psi<1$, the final displacement of nucleation phase is smaller than that of P wave. The difference in the amplitudes between the P wave and nucleation phase decreases when either s or γ increases and ψ decreases. The peak velocity of P wave on slider 2 decays with increasing μ, thus suggesting that the inertial effect is important on the rupture processes. Consequently, when $s>0.17$, $\gamma>1$, $1.15>\phi>1$, $\psi<1$, and $\mu<30$ simulation results exhibit the generation of nucleation phase on slider 1 and the formation of P wave on slider 2. The results are consistent with the observations and suggest the possibility of generation of nucleation phase on a sub-fault. This answer the question pointed out in this study.

Acknowledgments. The study was by Academia Sinica, the Ministry of Science and Technology, and the Central Weather Bureau, TAIWAN for financial support.

Nonlin. Processes Geophys. Discuss., https://doi.org/10.5194/npg-2018-49
Manuscript under review for journal Nonlin. Processes Geophys.
Discussion started: 5 December 2018

References

Andrews, D.J.: Rupture velocity of plane strain shear cracks, J. Geophys. Res., 81, 5679-5687, 1976.

Beeler, N.M.: Review of the physical basis of laboratory-derived relations for brittle failure and their implications for earthquake occurrence and earthquake nucleation, Pure Appl. Geophys. 161, 1853-1876, DOI:10.1007/s00024-004-2536-z, 2004.

Beroza, G.C. and Ellsworth, W.L.: Properties of the seismic nucleation phase, Tectonophys., 261, 209-227, 1996.

Brantut, N. Sulem, J., and Schubnel, A.: Effect of dehydration reactions on earthquake nucleation: Stable sliding, slow transients, and unstable slip, J. Geophys. Res., 116, B05304, doi:10.1029/2010JB007876, 2011.

Brune, J.: Implications of earthquake triggering and rupture propagation for earthquake prediction based on premonitory phenomena, J. Geophys. Res., 84, 2195-2198, 1979.

Burridge, R. and Knopoff, L.: Model and theoretical seismicity. Bull. Seism. Soc. Am., 57:341-371, 1967.

Campillo, M. and Ionescu, I.R.: Initiation of antiplane shear instability under slip dependent friction, J. Geophys. Res., 102, 20263-20371, 1997.

Carlson, J.M., Langer, J.S., Shaw, B.E., and Tang, C.: Intrinsic properties of a Burridge-Knopoff model of an earthquake fault, Phys. Rev. A., 44, 884-897, 1991.

Das, S. and Scholz, C.H.: Theory of time-dependent rupture in the Earth, J. Geophys. Res., 86(B7), 6039-6057, 1981.

Dieterich, J.H.: Modeling of rock friction 1. Experimental results and constitutive

Nonlin. Processes Geophys. Discuss., https://doi.org/10.5194/npg-2018-49
Manuscript under review for journal Nonlin. Processes Geophys.
Discussion started: 5 December 2018

equations, J. Geophys. Res., 84, 2161-2168, 1979.

Dieterich, J.H.: Potential for geophysical experiments in large scale tests, Geophys. Res. Letts., 8, 653-656, 1981.

Dieterich, J.H.: A model for the nucleation of earthquake slip, In Das et al. (eds.): Earthquake Source Mechanics, Geophysical Monograph 37, Maurice Ewing, AGU, 6, 37-47, 1986.

Dieterich, J.H.: Earthquake nucleation on faults with rate- and state-dependent strength, Tectonophys., 211, 115-134, 1992.

Ellsworth, W.L. and Beroza, G.C.: Seismic evidence for an earthquake nucleation phase, Science, 268, 851-855, 1995.

Ellsworth, W.L. and Beroza, G.C.: Observation of the seismic nucleation phase in the Ridgecrest, California, earthquake sequence, Geophys. Res. Letts., 25(3), 401-404, 1998.

Galvanetto, U.: Some remarks on the two-block symmetric Burridge–Knopoff model, Phys. Letts. A, 293, 251-259, 2002.

Iio, Y.: Slow initial phase of the P-wave velocity pulse generated by microearthquakes, Geophys. Res. Letts., 19, 477-480, 1992.

Iio, Y.: Observation of the slow initial phase of microearthquakes: Implications for earthquake nucleation and propagation, J. Geophys. Res., 100, 15333-15349, 1995.

Ionescu, I.R. and Campillo, M.: Influence of the shape of the friction law and fault finiteness on the duration of initiation, J. Geophys. Res., 104(B2), 3013-3024, 1999.

Kato, N., Yamamoto, K., and Hirasawa, T.: Microfracture processes in the breakdown zone during dynamic shear rupture inferred from laboratory observation of near-fault high frequency strong motion. Pure Appl. Geophys., 142, 713-734, 1994.

Kawamura, H., Yamamoto, M., and Ueda, Y.: Slow-slip phenomena represented by the one-dimensional Burridge–Knopoff model of earthquakes. J. Phys. Soc. Japan, 87, 053001, https://doi.org/10.7566/JPSJ.87.053001, 2018.

Kittel, C., Knight, W.D., and Ruderman, M.A.: Mechanics. Berkeley Physics Course, Vol. 1, McGraw-Hill Book Co., New York, NY, 480 pp, 1968.

Latour, S., Schubnel, A., Nielsen, S., Madariaga. R., and Vinciguerra, S.: Characterization of nucleation during laboratory earthquakes, Geophys. Res. Letts., 40, 5064-5069, doi:10.1002/grl.50974, 2013.

Lu, X. Rosakis, A.J. and Lapusta, N.: Rupture modes in laboratory earthquakes: Effect of fault prestress and nucleation conditions, J. Geophys. Res., 115. B12302, doi:10.1029/2009JB006833, 2010.

Mori, J. and Kanamori, H.: Initial rupture of earthquakes in the 1995 Ridgecrest, California sequence, Geophys. Res. Letts, 2, 2437-2440, 1996.

Ohnaka, M.: Earthquake source nucleation: a physical model for short-term precursors, Tectonophys., 211, 149-178, 1992.

Ohnaka, M. and Kuwahara, Y.: Characteristic features of local breakdown near a crack-tip in the transition zone from nucleation to dynamic rupture during stick-slip shear failure, Tectonophys., 175, 197-220, 1990.

Ohnaka, M. and Yamashita, T.: A cohesive zone model for dynamic shear faulting based on experimentally inferred constitutive relation and strong motion source parameters, J. Geophys. Res., 94, 4089-4104, 1989.

Ohnaka, M., Kuwahara, Y., and Yamamoto, K.: Constitutive relations between dynamic physical parameters near a tip of the propagating slip zone during stick-slip shear failure, Tectonophys., 144, 109-125, 1987.

Nonlin. Processes Geophys. Discuss., https://doi.org/10.5194/npg-2018-49
Manuscript under review for journal Nonlin. Processes Geophys.
Discussion started: 5 December 2018

Nonlinear Processes in Geophysics
Discussions
Open Access

Press, W.H., Flannery, B.P., Teukolsky, S.A., and Vetterling, W.T.: Numerical Recipes, Cambridge Univ. Press, Cambridge, 818 pp, 1986.

Rice, J.R.: Heating and weakening of faults during earthquake slip, J. Geophys. Res., 111, B05311, doi:10.1029/2005JB004006, 2006.

Rice, J.R., Lapusta, N., and Ranjith, K.: Rate and state dependent friction and the stability of sliding between elastically deformable solids, J. Mech. Phys. Solids, 49, 1865-1898, 2001.

Roy, M. and Marone, C.: Earthquake nucleation on model faults with rate- and state-dependent friction: Effects of inertia, J. Geophys. Res., 101(B6), 13919-13932, 1996.

Ruiz. S., Aden-Antoniow. F., Baez, J.C., Otarola, C., Potin, B., del Campo, F., Poli, P., Flores, C., Satriano. C., Leyton, F., Madariaga, R., and Bernard, P.: Nucleation phase and dynamic inversion of the M_w6.9 Valparaíso 2017 earthquake in Central Chile, Geophys. Res. Letts., 44, 10290-10297, doi.org/10.1002/ 2017GL075675, 2017.

Scholz, C.H., Molnar, P., and Johnson, T.: Detailed studies of frictional sliding of granite and implications for the earthquake mechanism, J. Geophys. Res., 77, 6392- 6400, 1972.

Schmitt, S.V., Segall, P., and Dunham, E.M.: Nucleation and dynamic rupture on weakly stressed faults sustained by thermal pressurization, J. Geophys. Res. Solid Earth, 120, 7606-7640, doi:10.1002/2015JB012322, 2015.

Segall, P. and Rice, J.R.:. Does shear heating of pore fluid contribute to earthquake nucleation?, J. Geophys. Res., 111, B09316, doi:10.1029/2005JB004129, 2006.

Shibazaki, B. and Matsu'ura, M.: Spontaneous processes for nucleation, dynamic propagation, and stop of earthquake rupture, Geophys. Res. Lett., 19, 1189-1192,

Nonlin. Processes Geophys. Discuss., https://doi.org/10.5194/npg-2018-49
Manuscript under review for journal Nonlin. Processes Geophys.
Discussion started: 5 December 2018

1992.

Shibazaki, B. and Matsu'ura, M.: Transition process from nucleation to high-speed rupture propagation: Scaling from stick-slip experiments to natural earthquakes (abstract), Eos, Trans., AGU, 47, 410, 1993.

Shibazaki, B. and Matsu'ura, M.: Foreshocks and pre-events associated with the nucleation of large earthquakes, Geophys. Res. Letts., 22(10), 1305-1308, 1995.

Tal, Y., Hager, B.H., and Ampuero, J.P.: The effects of fault roughness on the earthquake nucleation process, J. Geophys. Res., 123, 437-456 doi.org/10.1002/ 2017JB014746, 2018.

Turcotte, D.L.: Fractals and Chaos in Geology and Geophysics, Cambridge Univ. Press Cambridge, 221pp, 1992

Ueda, Y., Morimoto, S., Kakui, S., Yamamoto, T., and Kawamura, H.: Nucleation process in the Burridge-Knopoff model of earthquakes, Europhys. Lett., 106, 69001, doi:10.1209/0295-5075/106/69001, 2014.

Ueda, Y., Morimoto, S., Kakui, S., Yamamoto, T., and Kawamura, H.: Dynamics of nucleation process represented by the Burridge-Knopoff model, Eur. Phys. J. B, 88, 235, DOI:10.1140/epjb/e2015-60499-0, 2015.

Umeda, Y.: High-amplitude seismic waves radiated from the bright spot of an earthquake, Tectonophys., 135, 81-92, 1990.

Wang, J.H.: Effect of seismic coupling on the scaling of seismicity, Geophys. J. Int., 121, 475-488, 1995.

Wang, J.H.: Stability analysis of slip of a one-body spring-slider model in the presence of thermal pressurization, Ann. Geophys., 56(3), R03332, doi:10.4401/ ag-5548, 2013.

Wang, J.H.: Slip of a one-body spring-slider model in the presence of slip-weakening

Nonlin. Processes Geophys. Discuss., https://doi.org/10.5194/npg-2018-49
Manuscript under review for journal Nonlin. Processes Geophys.
Discussion started: 5 December 2018

friction and viscosity, Ann. Geophys., 59(5), S0541, doi:10.4401/ ag-7063, 2016.

Wang, J.H.: Frictional and viscous effects on the nucleation phase of an earthquake nucleation, J. Seismol., 21(6), 1517-1539, 2017a.

Wang, J.H.: Slip of a two-degree-of-freedom spring-slider model in the presence of slip-weakening friction and viscosity, Ann. Geophys., 60(6), S0659, doi:10. 4401/ag-7295, 2017b.

Wells, D.L. and Coppersmith, K.J.: New empirical relationships among magnitude, rupture length, rupture width, rupture area, and surface displacement, Bull. Seism. Soc. Am., 84, 974-1002, 1994.

Nonlin. Processes Geophys. Discuss., https://doi.org/10.5194/npg-2018-49
Manuscript under review for journal Nonlin. Processes Geophys.
Discussion started: 5 December 2018

Nonlinear Processes in Geophysics
Discussions
Open Access

List of Figure Captions

Figure 1. An example to show the nucleation phase, onset of the *P* wave, and the *P* wave in velocity seismogram.

Figure 2. A two-body spring-slider model: F_i=the friction force at the *i*-th slider, m_i=the mass of the *i*-th slider, *K*=the stiffness between two sliders, L_i=the stiffness between the *i*-th slider and the moving plate, C_i=the viscosity coefficient between the *i*-th slider and the moving plate, and v_p=the velocity of the moving plate, and u_i (*i*=1, 2) is the displacement of the *i*-th slider.

Figure 3. The variations of friction force with sliding displacement for u_c=0.1, 0.3, 0.5, 0.7, and 0.9 m when F_o=1 unit.

Figure 4. The time sequences of V/V_{max} and U/U_{max}: (a) for *s*=0.06, (b) for *s*=0.12, (c) for *s*=0.30, and (d) for *s*=0.48 when μ=1, f_{o1}=1.0 and f_{o2}=1.0 (with ϕ=1), U_{c1}=0.5 and U_{c2}=0.5 (with ψ=1), and η_1=0 and η_2=0 (with γ=1).

Figure 5. The time sequences of V/V_{max} and U/U_{max}: (a) for γ=0.00, (b) for γ=0.01, (c) for γ=0.05, and (d) for γ=0.10 when *s*=0.48, μ=1, η_1=10, f_{o1}=1.0 and f_{o2}=1.0 (with ϕ=1), and U_{c1}=0.5 and U_{c2}=0.5 (with ψ=1).

Figure 6. The time sequences of V/V_{max} and U/U_{max}: (a) for γ=0.00, (b) for γ=0.01, (c) for γ=0.05, and (d) for γ=0.10 when *s*=0.48, μ=1, η_1=10, f_{o1}=1.0 and f_{o2}=1.1 (with ϕ=1.1), and U_{c1}=0.5 and U_{c2}=0.5 (with ψ=1).

Figure 7. The time sequences of V/V_{max} and U/U_{max}: (a) for γ=0.00, (b) for γ=0.01, (c) for γ=0.05, and (d) for γ=0.10 when *s*=0.48, μ=1, η_1=10, f_{o1}=1.0 and f_{o2}=1.1 (with ϕ=1.1), and U_{c1}=0.5 and U_{c2}=0.1 (with ψ=0.2).

Figure 8. The time sequences of V/V_{max} and U/U_{max}: (a) for γ=0.00, (b) for γ=0.01, (c) for γ=0.05, and (d) for γ=0.10 when *s*=0.17, μ=1, η_1=10, f_{o1}=1.0 and f_{o2}=1.1

Nonlin. Processes Geophys. Discuss., https://doi.org/10.5194/npg-2018-49
Manuscript under review for journal Nonlin. Processes Geophys.
Discussion started: 5 December 2018

Nonlinear Processes in Geophysics Discussions

(with ϕ=1.1), and U_{c1}=0.5 and U_{c2}=0.1 (with ψ=0.2).

Figure 9. The time sequences of V/V_{max} and U/U_{max}: (a) for μ=1, (b) for μ=5, (c) for μ=10, and (d) for μ=30 when s=0.48, f_{o1}=1.0 and f_{o2}=1.1 (with ϕ=1.1), U_{c1}=0.5 and U_{c2}=0.1 (with ψ=0.2), and η_1=10 and η_2=0 (with γ=0).

Figure 10. The time sequences of V/V_{max} and U/U_{max}: (a) for μ=1, (b) for μ=5, (c) for μ=10, and (d) for μ=30 when s=0.17, f_{o1}=1.0 and f_{o2}=1.1 (with ϕ=1.1), U_{c1}=0.5 and U_{c2}=0.1 (with ψ=0.2), and η_1=10 and η_2=0 (with γ=0).

Nonlin. Processes Geophys. Discuss., https://doi.org/10.5194/npg-2018-49
Manuscript under review for journal Nonlin. Processes Geophys.
Discussion started: 5 December 2018

Nonlinear Processes in Geophysics
Discussions

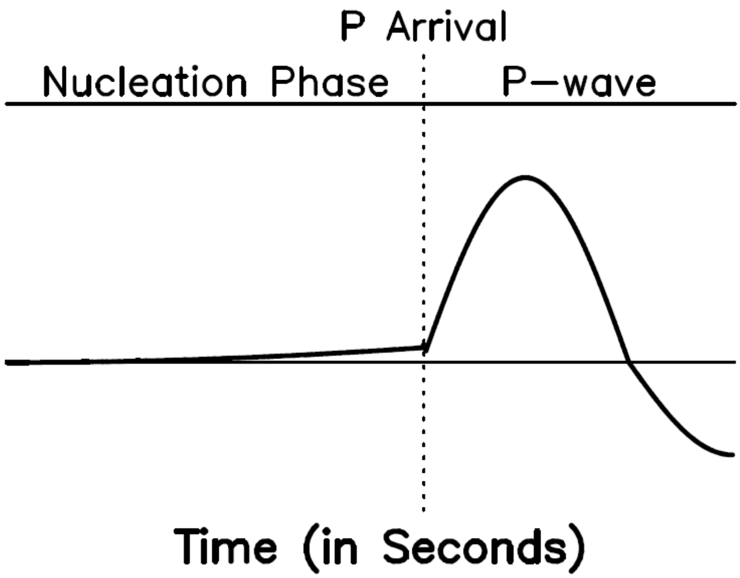

Figure 1. An example to show the nucleation phase, onset of the *P* wave, and the *P* wave in velocity seismogram.

Nonlin. Processes Geophys. Discuss., https://doi.org/10.5194/npg-2018-49
Manuscript under review for journal Nonlin. Processes Geophys.
Discussion started: 5 December 2018

Nonlinear Processes in Geophysics
Discussions

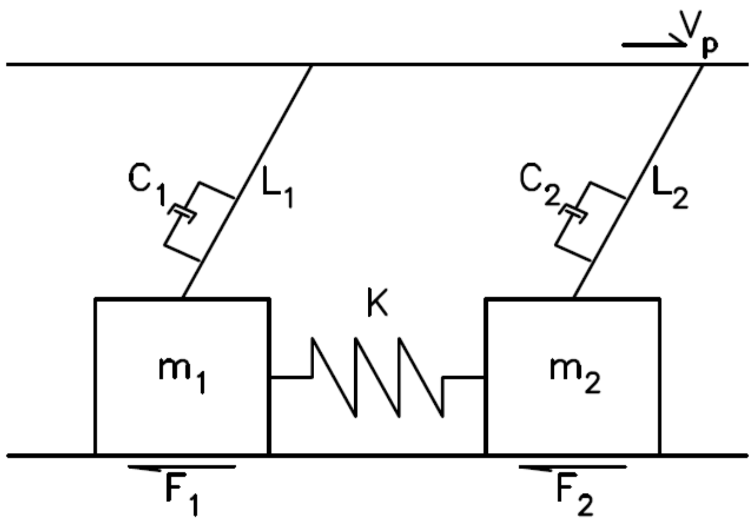

Figure 2. A two-body spring-slider model: F_i=the friction force at the *i*-th slider, m_i=the mass of the *i*-th slider, K=the stiffness between two sliders, L_i=the stiffness between the *i*-th slider and the moving plate, C_i=the viscosity coefficient between the *i*-th slider and the moving plate, and v_p=the velocity of the moving plate, and u_i (i=1, 2) is the displacement of the *i*-th slider.

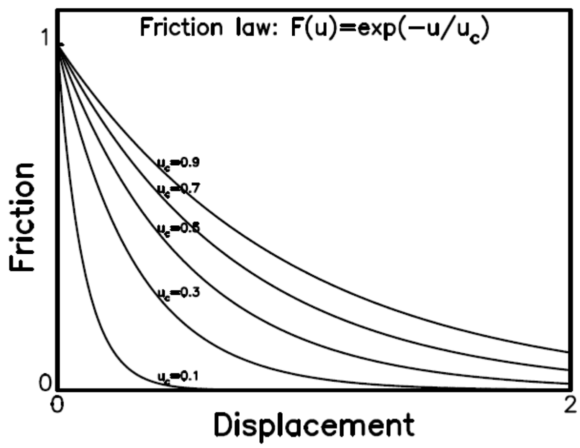

Figure 3. The variations of friction force with sliding displacement for u_c=0.1, 0.3, 0.5, 0.7, and 0.9 m when F_o=1 unit.

Nonlin. Processes Geophys. Discuss., https://doi.org/10.5194/npg-2018-49
Manuscript under review for journal Nonlin. Processes Geophys.
Discussion started: 5 December 2018

Nonlinear Processes in Geophysics
Discussions
Open Access
EGU

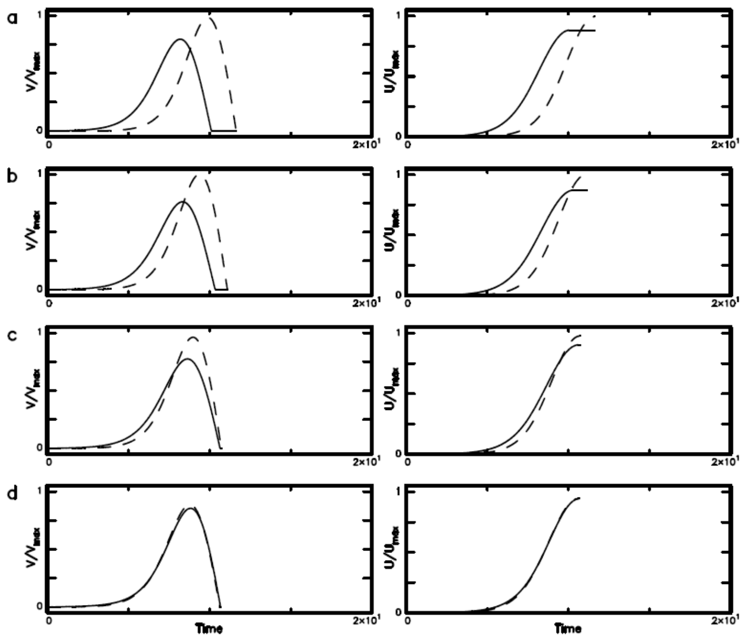

Figure 4. The time sequences of V/V_{max} and U/U_{max}: (a) for s=0.06, (b) for s=0.12, (c) for s=0.30, and (d) for s=0.48 when μ=1, f_{o1}=1.0 and f_{o2}=1.0 (with ϕ=1), U_{c1}=0.5 and U_{c2}=0.5 (with ψ=1), and η_1=0 and η_2=0 (with γ=1).

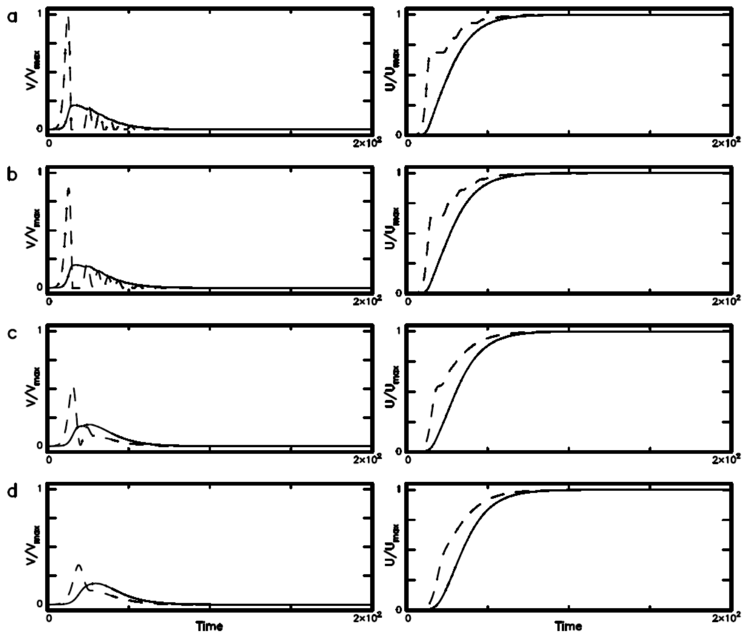

Figure 5. The time sequences of V/V_{max} and U/U_{max}: (a) for γ=0.00, (b) for γ=0.01, (c) for γ=0.05, and (d) for γ=0.10 when s=0.48, μ=1, η_1=10, f_{o1}=1.0 and f_{o2}=1.0 (with ϕ=1), and U_{c1}=0.5 and U_{c2}=0.5 (with ψ=1).

Nonlin. Processes Geophys. Discuss., https://doi.org/10.5194/npg-2018-49
Manuscript under review for journal Nonlin. Processes Geophys.
Discussion started: 5 December 2018

Nonlinear Processes in Geophysics
Discussions
Open Access

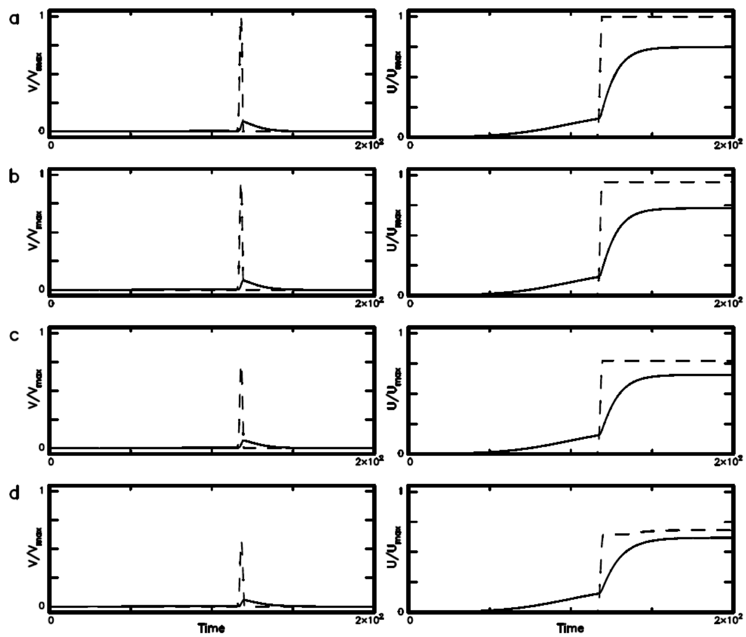

Figure 6. The time sequences of V/V_{max} and U/U_{max}: (a) for γ=0.00, (b) for γ=0.01, (c) for γ=0.05, and (d) for γ=0.10 when s=0.48, μ=1, η_1=10, f_{o1}=1.0 and f_{o2}=1.1 (with ϕ=1.1), and U_{c1}=0.5 and U_{c2}=0.5 (with ψ=1).

Nonlin. Processes Geophys. Discuss., https://doi.org/10.5194/npg-2018-49
Manuscript under review for journal Nonlin. Processes Geophys.
Discussion started: 5 December 2018

Nonlinear Processes in Geophysics
Discussions
Open Access

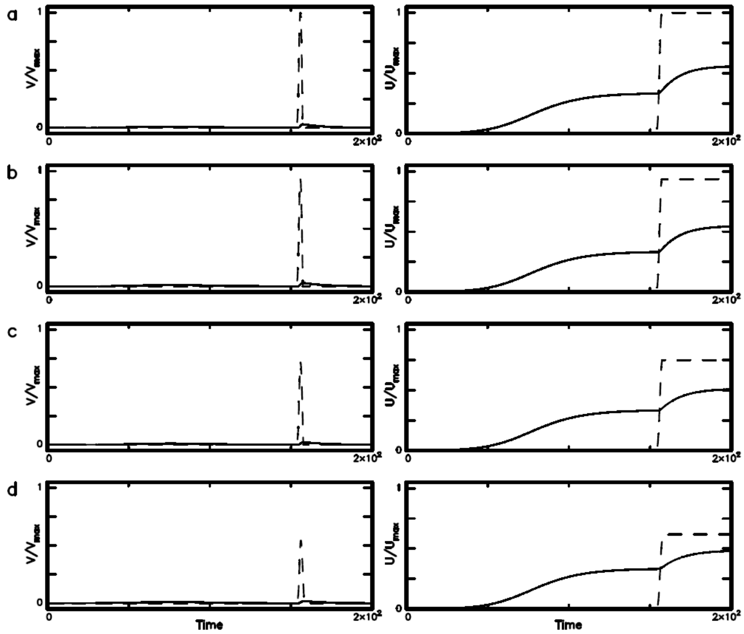

Figure 7. The time sequences of V/V_{max} and U/U_{max}: (a) for γ=0.00, (b) for γ=0.01, (c) for γ=0.05, and (d) for γ=0.10 when s=0.48, μ=1, η_1=10, f_{o1}=1.0 and f_{o2}=1.1 (with ϕ=1.1), and U_{c1}=0.5 and U_{c2}=0.1 (with ψ=0.2).

Nonlin. Processes Geophys. Discuss., https://doi.org/10.5194/npg-2018-49
Manuscript under review for journal Nonlin. Processes Geophys.
Discussion started: 5 December 2018

Nonlinear Processes in Geophysics
Discussions
Open Access

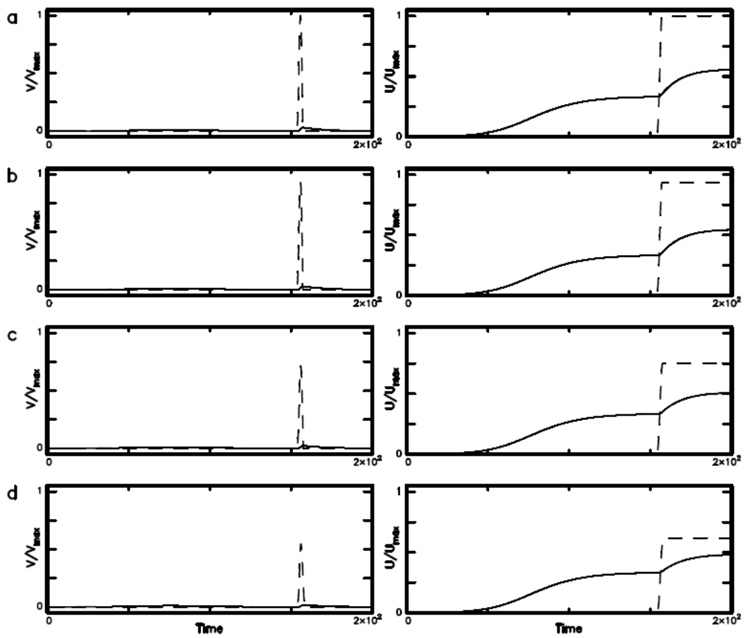

Figure 8. The time sequences of V/V_{max} and U/U_{max}: (a) for γ=0.00, (b) for γ=0.01, (c) for γ=0.05, and (d) for γ=0.10 when s=0.17, μ=1, η_1=10, f_{o1}=1.0 and f_{o2}=1.1 (with ϕ=1.1), and U_{c1}=0.5 and U_{c2}=0.1 (with ψ=0.2).

Nonlin. Processes Geophys. Discuss., https://doi.org/10.5194/npg-2018-49
Manuscript under review for journal Nonlin. Processes Geophys.
Discussion started: 5 December 2018

Nonlinear Processes in Geophysics
Open Access
Discussions

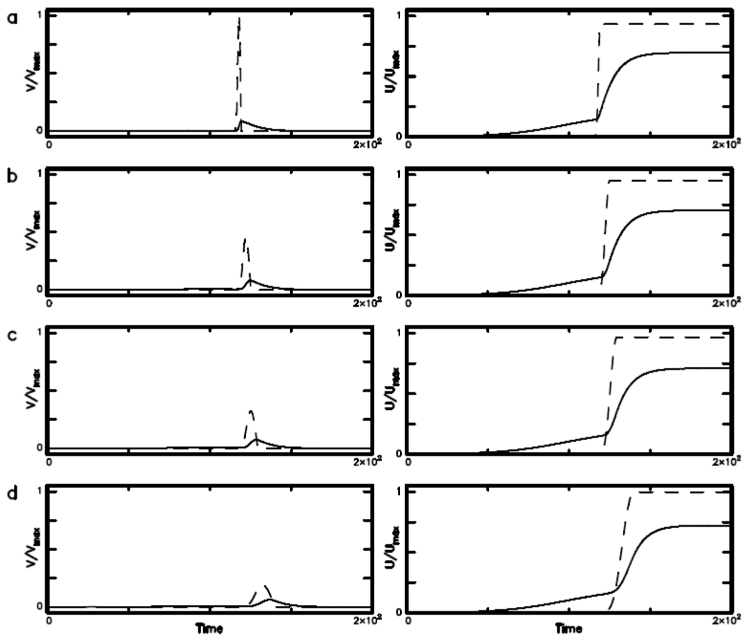

Figure 9. The time sequences of V/V_{max} and U/U_{max}: (a) for μ=1, (b) for μ=5, (c) for μ=10, and (d) for μ=30 when s=0.48, f_{o1}=1.0 and f_{o2}=1.1 (with ϕ=1.1), U_{c1}=0.5 and U_{c2}=0.1 (with ψ=0.2), and η_1=10 and η_2=0 (with γ=0).

Nonlin. Processes Geophys. Discuss., https://doi.org/10.5194/npg-2018-49
Manuscript under review for journal Nonlin. Processes Geophys.
Discussion started: 5 December 2018

Nonlinear Processes in Geophysics
Discussions
Open Access

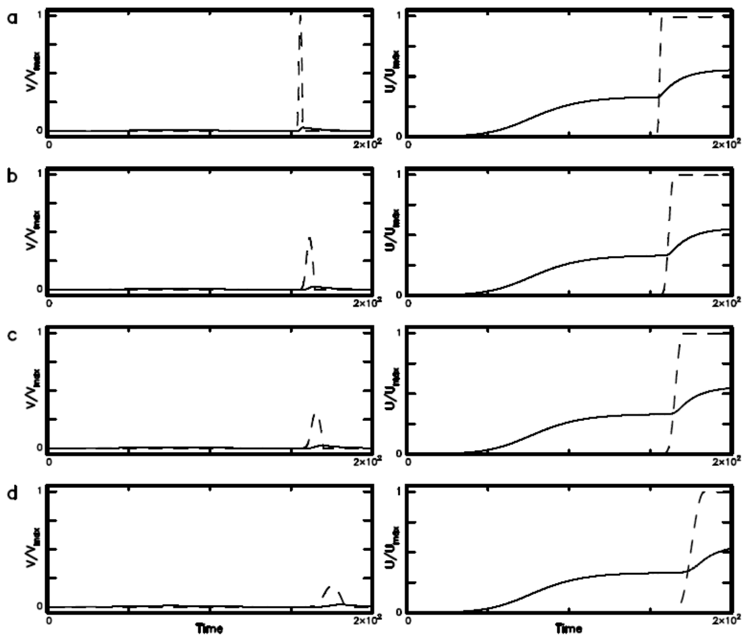

Figure 10. The time sequences of V/V_{max} and U/U_{max}: (a) for μ=1, (b) for μ=5, (c) for μ=10, and (d) for μ=30 when s=0.17, f_{o1}=1.0 and f_{o2}=1.1 (with ϕ=1.1), U_{c1}=0.5 and U_{c2}=0.1 (with ψ=0.2), and η_1=10 and η_2=0 (with γ=0).